

Water Resources Research

RESEARCH ARTICLE

10.1029/2018WR023567

Key Points:

- There is significant spatial heterogeneity in extreme rainfall across the Baltimore area, which is closely linked to the complex terrain
- Stochastic storm transposition-based analysis highlights the necessity of considering spatial heterogeneity in rainfall estimation

Supporting Information:

- Supporting Information S1

Correspondence to:

Z. Zhou and S. Liu,
zhouzz@tongji.edu.cn;
liusliu@tongji.edu.cn

Citation:

Zhou, Z., Smith, J. A., Wright, D. B., Baeck, M. L., Yang, L., & Liu, S. (2019). Storm catalog-based analysis of rainfall heterogeneity and frequency in a complex terrain. *Water Resources Research*, 55, 1871–1889. <https://doi.org/10.1029/2018WR023567>

Received 27 JUN 2018

Accepted 31 JAN 2019

Accepted article online 12 FEB 2019

Published online 4 MAR 2019

Storm Catalog-Based Analysis of Rainfall Heterogeneity and Frequency in a Complex Terrain

Zhengzheng Zhou^{1,2} , James A. Smith² , Daniel B. Wright³ , Mary Lynn Baeck², Long Yang^{2,5} , and Shuguang Liu⁴ 

¹State Key Laboratory of Marine Geology, School of Ocean and Earth Science, Tongji University, Shanghai, China, ²Department of Civil and Environmental Engineering, Princeton University, Princeton, NJ, USA, ³Department of Civil and Environmental Engineering, University of Wisconsin, Madison, WI, USA, ⁴Department of Hydraulic Engineering, Tongji University, Shanghai, China, ⁵School of Geographic and Oceanic Science, Nanjing University, Nanjing, Jiangsu Province, China

Abstract Urban development, topographic relief, and coastal boundaries can all exert influences on storm hydroclimatology, making rainfall and flood frequency analysis a major challenge. This study explores heterogeneity in extreme rainfall in the Baltimore Metropolitan region at small spatial scales using hydrometeorological analyses of major storm events in combination with hydroclimatological analyses based on *storm catalogs* developed using a 16-year record of high-resolution bias-corrected radar rainfall fields. Our analyses demonstrate the potential for rainfall frequency methods using storm catalogs combined with stochastic storm transposition (SST); procedures are implemented for Dead Run, a small (14.3 km^2) urban watershed located within the Baltimore Metropolitan area. The results point to the pronounced impact of complex terrain (including the Chesapeake Bay to the east, mountainous terrain to the west and urbanization in the region) on the regional rainfall climatology. Warm-season thunderstorm systems are shown to be the dominant mechanism for generating extreme, short-duration rainfall that leads to flash flooding. The SST approach is extended through the implementation of a *multiplier field* that accounts for spatial heterogeneities in extreme rainfall magnitude. SST-based analyses demonstrate the need to consider rainfall heterogeneity at multiple scales when estimating the rainfall intensity-duration-frequency relationships.

1. Introduction

Rainfall and flood frequency analyses are central to hydrologic engineering design and probabilistic flood hazard assessment. Conventional approaches rely on multidecadal records of rainfall or streamflow from one or more gauge locations. In many settings, particularly urban areas, records are either nonexistent or of questionable validity due to the impacts of urbanization on the rainfall and flood hydroclimatology (Khaliq et al., 2006; Milly et al., 2008; Villarini et al., 2010). Furthermore, rainfall frequency analyses, and so-called *design storm* flood frequency analyses based upon them, typically simplify the spatial and temporal representation of extreme rainfall at the watershed scale. Previous studies have shown, however, that rainfall space-time structure plays an important role in flood generation in urban watersheds, where heterogeneity in land use/land cover complicates the translation of rainfall spatiotemporal distribution into flood response (Morin et al., 2006; Ogden et al., 2000; Ramos et al., 2005; Zhou et al., 2017). This suggests that design storm approaches may not be appropriate in such catchments (Wright, Smith, Villarini, et al., 2014). Moreover, many urban watersheds are embedded within heterogeneous large-scale physiographic settings, often including topographic features, land-water boundaries, and a range of land surface and land use types (Smith, Baeck, et al., 2011; Tarolli et al., 2013; Yang et al., 2013), all of which can exert local-to-regional scale influences on the extreme rainfall climatology (Shepherd, 2005; see also Norbiato et al., 2007; Smith et al., 2007; Yang et al., 2014).

Long-term records (10 or more years) of high-resolution bias-corrected radar rainfall fields are valuable for studies of urban rainfall (Hamidi et al., 2017; Smith et al., 2012; Thorndahl et al., 2014) and flooding (Javier et al., 2007; Smith et al., 2007; Villarini et al., 2010; Wright, Smith, & Baeck, 2014), since they resolve fine-scale spatial and temporal structures of extreme rainfall. *Storm catalogs* of radar rainfall fields can provide the observational resource for examining spatial heterogeneity of extreme rainfall over small spatial scales (1- to 100-km length scales), which is challenging with all but the densest rain gauge networks. When coupled with stochastic storm transposition (SST), storm catalogs offer interesting opportunities for rainfall and flood frequency analysis.

SST was developed as an alternative approach for assessing the frequency of extreme rainfall and flooding (Alexander, 1963; Fontaine & Potter, 1989; Foufoula-Georgiou, 1989; Wilson & Foufoula-Georgiou, 1990; Wright et al., 2013, 2017). The main idea of SST is to use a record of observed storms over a region to better inform estimates of rainfall frequency at a location of interest (such as a watershed) within the region, with the fundamental assumption being that a storm that occurred elsewhere within the region could have occurred at the location of interest. Like other rainfall or streamflow regionalization techniques (e.g., Dawdy et al., 2012), SST uses regional probabilistic resampling combined with storm geospatial translation (transposition) to estimate local-scale extreme event frequency. Foufoula-Georgiou (1989) investigated an SST approach as a possible methodology of assessing the probability of exceedance of extreme precipitation depths over a catchment. This frequency analysis approach has been used for rainfall (Wilson & Foufoula-Georgiou, 1990) and floods (Franchini et al., 1996; Gupta, 1972). Nathan et al. (2016) developed a dimensionless SST approach relying on a gridded data set of gauge-based daily rainfall and applied to two large catchments in the southern Australia. These studies, however, were limited by the lack of long-term records of high-resolution rainfall data, while SST methods generally face limitations in regions with complex rainfall climatology (England et al., 2014). Wright et al. (2013) and Wright, Smith, Villarini, et al. (2014) introduced an SST framework that utilizes high-resolution radar rainfall fields for rainfall and flood frequency analysis and used the technique in the Charlotte, North Carolina Metropolitan region in the United States. These studies show that SST with 10 years of radar rainfall data can produce satisfactory frequency analysis results that have desirable properties not provided by conventional methods. In particular, Wright, Smith, Villarini, et al. (2014) coupled SST with a distributed hydrologic model to examine the role that rainfall spatiotemporal distribution plays in determining multiscale flood frequency, which is beyond the capabilities of standard design storm methods.

Previous SST studies have been relatively simplistic in their consideration of spatial heterogeneity in the extreme rainfall hydroclimatology, often, for example, assuming a uniform probability of storm occurrence everywhere (Fontaine & Potter, 1989; Franchini et al., 1996). Several studies have discussed the nonuniform probability distribution of location of storm center (England et al., 2014; Foufoula-Georgiou, 1989; Wright et al., 2017). In this study, we expand the framework of SST approach by explicitly considering the spatial heterogeneities in both storm occurrence and storm magnitude. Due to the complex terrain in the Baltimore region, the spatial heterogeneity in the short-duration extreme rainfall will be explored in detail and its impact on SST estimation will be addressed.

The two main objectives of our study are to characterize spatial heterogeneity in the extreme rainfall climatology over small spatial scales across the Baltimore Metropolitan region near the mid-Atlantic coast of the United States and to develop SST-based rainfall frequency analyses for Dead Run, a 14.3 km^2 urban watershed within the Baltimore region. Our approaches for addressing these objectives center on analyses of a 16-year high-resolution record of bias-corrected radar rainfall (Smith et al., 2012). Our analyses build on previous empirical and modeling studies showing pronounced rainfall heterogeneities in the region due to complex terrain (Figure 1a and see the details in section 2.1) and urban impacts on rainfall. We first characterize the key feature of space-time variation of heavy rainfall through climatological analyses of a large population of storms identified using radar-based storm catalogs and through detailed analyses of two major storm events. We then move on to expand the SST approach to account for spatial heterogeneities in extreme rainfall magnitude.

The paper is organized as follows: in section 2, we first introduce the study region and data and then describe the SST-based methodology, storm type identification, and comparison of estimations; on section 3, the results of the regional extreme rainfall heterogeneity and SST-based rainfall frequency analyses are presented. A summary and conclusions are presented in section 4.

2. Data and Methods

2.1. Study Region

This study focuses on the Baltimore Metropolitan region, which is characterized by contrasts in topography, land use, and land cover and also by the land-water boundary along the Chesapeake Bay (Smith et al., 2012; Figure 1). The Fall Line is the transition zone between the Piedmont and Coastal Plain physiographic

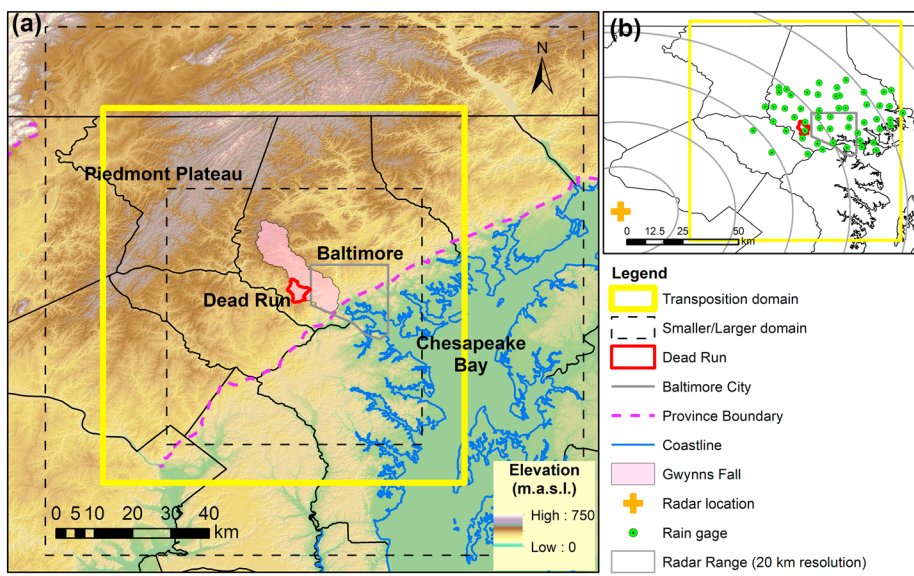


Figure 1. Location of the Baltimore study region and the Dead Run study watershed.

provinces (Reger & Cleaves, 2008); it divides the region into two topographic zones, the upland Piedmont Plateau to the northwest and lowland Coastal Plain to the southeast (Ntelekos et al., 2008). Urban development along much of the eastern United States is concentrated along the Fall Line, which passes through the Baltimore City and the lower portion of the Gwynns Falls watershed, the principal study watershed of the Baltimore Ecosystem Study, a Long Term Ecological Research project focusing on the ecology and hydrology of the urban environment (Groffman et al., 2003; Smith, Miller, et al., 2005; Welty et al., 2007). The *Bay Breeze* circulation of the Chesapeake Bay is an important element of the hydroclimatology of extreme warm season rainfall in the region (Ryu et al., 2016).

Rainfall analyses are focused on Dead Run, a highly urbanized 14.3 km^2 watershed that is a tributary to the Gwynns Falls and is located west of Baltimore City. The basin has an impervious fraction of approximately 52.3%. Fifty-four rain gauges in and around the Baltimore City are available for bias correction of radar data. The region also has a dense network of stream gauges connected to Baltimore Ecosystem Study hydrologic monitoring activities. The wealth of data for the Dead Run watershed provides exceptional observational resources to examine urban hydrology. Previous studies have examined the rainfall and hydrologic response of Dead Run (Beighley & Moglen, 2002; Meierdiercks et al., 2010; Nelson et al., 2006; Smith, Miller, et al., 2005; Smith et al., 2015), which has experienced a major flood event on 7 July 2004 (Javier et al., 2007; Ntelekos et al., 2008).

2.2. Radar Rainfall Fields

Two-dimensional Cartesian radar rainfall fields are estimated using volume scan reflectivity observations from the Sterling, Virginia WSR-88D (Weather Surveillance Radar-1988 Doppler) radar. The Hydro-NEXRAD algorithms (Krajewski et al., 2011; Seo et al., 2011) that have been used in previous extreme rainfall hydroclimatological studies (Javier et al., 2007; Lin et al., 2010; Smith et al., 2007; Smith, Baeck, et al., 2011; Villarini et al., 2013; Volkmann et al., 2010; Wright et al., 2012) are used to estimate rainfall from reflectivity fields. The Sterling radar is approximately 70 km from Dead Run (Figure 1b). These rainfall fields have a temporal resolution of 15-min and spatial resolution of 1 km^2 for the 2000–2015 period.

A mean-field bias correction is applied on a daily (12 to 12 UTC) basis using a network of rain gauges in and around the Baltimore County (Figure 1). Mean-field bias correction removes systematic spatial and temporal biases due to variability in Z-R relationships and radar calibration errors (Fulton et al., 1998; Smith & Krajewski, 1991; Villarini & Krajewski, 2010). The bias computation takes the form

$$B_i = \frac{\sum_{S_i} G_{ij}}{\sum_{S_i} R_{ij}} \quad (1)$$

where G_{ij} is the rainfall accumulation for gauge j on day i , R_{ij} is the daily rainfall accumulation for the collocated radar pixel accumulation on day i , and S_i is the index of the rain gauge stations for which both the rain gauge and the radar report positive rainfall accumulations for day i . The bias value B_i is set to be different from 1.0 only if there are at least five positive radar-rain gauge pairs in the domain and at least 80 (out of 96) 15-min radar fields for a day. Each 15-min radar rainfall field from day i is then multiplied by B_i . The mean-field bias correction procedure is the same as that used in previous hydrologic studies in Smith and Krajewski (1991), Seo and Breidenbach (2002), Smith et al. (2002), Wright et al. (2012), Wright, Smith, & Baeck (2014).

2.3. SST Procedure

Storm catalogs and SST analyses in this study use RainyDay, an open-source SST software package (Wright et al., 2017). The following steps describe briefly the approach for rainfall frequency analysis in the Dead Run watershed, while the reader is directed to Wright et al. (2017) and references therein for further details.

The first step is to identify a geospatial *transposition domain* that contains the watershed of interest. This domain can be rectangular or of arbitrary shape. Most of the results in this study were generated using a square 7,000-km² transposition domain centered on the Dead Run watershed. Sensitivity analyses presented in section 3.4 assess the role of domain size on SST results. Rainfall fields should be examined to assess spatial heterogeneities in extreme rainfall over the transposition domain. Direct analyses of rainfall fields can be used to characterize spatial heterogeneities in storm occurrence and rainfall magnitudes, along with spatial heterogeneities or anisotropy in spatial correlation structure of rainfall fields. Analyses of cloud-to-ground lightning climatology is useful for assessing spatial heterogeneities of thunderstorms (see Ntelekos et al., 2007). Analyses in section 3.1 will show that this domain exhibits significant heterogeneity.

The second step is to identify the largest m temporally nonoverlapping storms within the domain at the t -hour time scale. This set of storms is referred to as a *storm catalog*. Since the goal of the procedure is to estimate rainfall and flood exceedance probabilities for a specific watershed, the m largest storms are selected with respect to the size, shape, and orientation of that watershed. For example, the principal axis of Dead Run is orientated roughly west-east and has an area of 14.3 km², so the m storms that constitute the t -hour storm catalog are those associated with high t -hour rainfall intensities over an area of 14.3 km² with the same shape and orientation as Dead Run. We henceforth refer to these as *DR-shaped storms*. Since the size of radar grid cell is 1 km², the DR-shaped area constitutes 16 grid cells. The m DR-shaped storms are selected from an n -year rainfall record, such that an average of $\lambda = m/n$ storms per year are included in the storm catalog. Low exceedance probability events are relatively insensitive to storm catalog size, but a large catalog can help to improve the estimation of more frequent events (Wright et al., 2013). Wright et al. (2017) suggests that $\lambda \geq 10$ is a good starting point for new analyses. In this study, we chose $m = 200$ storms over the 16-year radar record and create storm catalogs for durations of $t = 1, 3$, and 6 hr. Sensitivity to the choice of m is examined in section 3.4. If two or more distinct t -hour periods of heavy rainfall occurred within 24 hr, only the period with the highest rainfall rate is included in the storm catalog.

The third step is to randomly sample a subset of k storms from the storm catalog for a 1-year period. Most SST studies assume that storm counts have a Poisson distribution with rate of occurrence $\lambda = m/n$ storms per year (Foufoula-Georgiou, 1989; Gupta, 1972; Suyanto et al., 1995). This assumption is used in this study, leading to $\lambda = 12.5$ storms per year.

For each of the k storms, all associated rainfall fields are transposed by an east-west distance Δx and a north-south distance Δy . Δx and Δy are drawn from distributions $D_X(x)$ and $D_Y(y)$, which are bounded by the limits of the transposition domain. The motion and evolution of the storm at all periods are thus unaltered during transposition, and only the location is changed. This step is illustrated schematically in Figure 2 for four successive 15-min time periods. Based on the spatial heterogeneity analysis of extreme rainfall in the domain, distributions $D_X(x)$ and $D_Y(y)$ can be set as uniform or nonuniform. The latter option is used in this study, since the assumption of regional homogeneity cannot be relaxed in the Baltimore area (see section 3.1.1 for more details). A two-dimensional probability density function of spatial storm occurrence (Wright

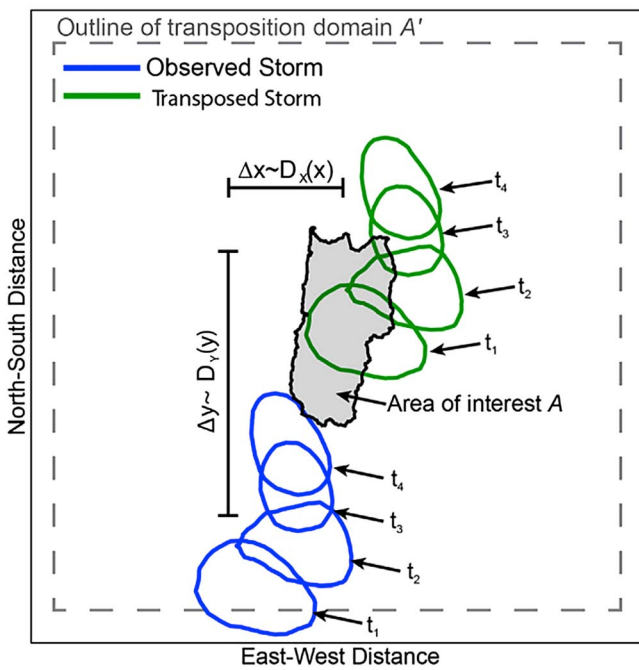


Figure 2. Depiction of stochastic storm transposition procedure for a single storm consisting of four time intervals. The gray area in the center is the target watershed, and dashed line is the boundary of transposition domain. The blue ellipses show the time evolution of an arbitrary rainfall isohyet, while the green ellipses show the time evolution of transposed rainfall isohyets. (Reprinted from Wright et al., 2017).

effectively expand the sample size, especially for the upper tail. Although the above steps constitute a resampling technique akin to bootstrapping using regional storm observations that can be viewed as a bootstrapping technique, *resampling* is used to highlight the regional nature of the method. In this study, these steps are repeated 500 times and the ordered *annual* maxima are used to generate rainfall return period estimates up to 500 years. One thousand such realizations of 500-year series are generated, and the median value of 1,000 realizations is set as the estimates for each return period.

2.4. Storm Classification

Individual storm events within a storm catalog can be classified according to the type of weather system that produced them. Classification can be useful in the context of rainfall and flood frequency analysis, since in

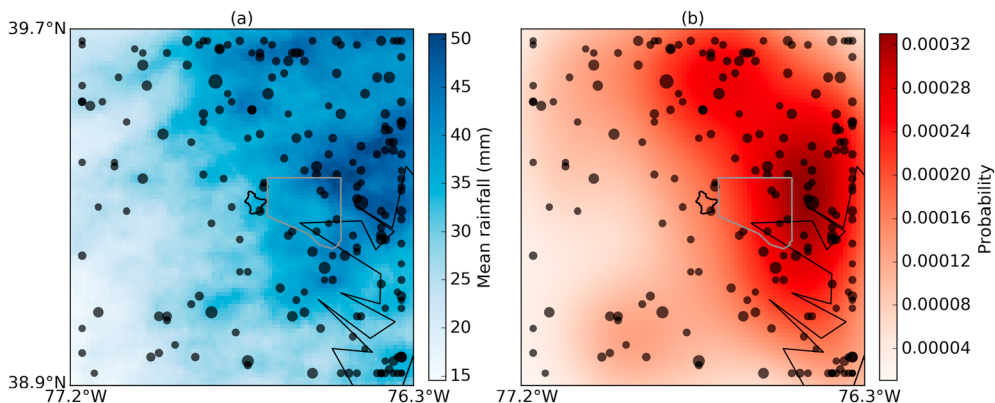


Figure 3. Maps of mean storm total rainfall (a) and probability of storm occurrence (b) for the 200 storms in the 3-hr storm catalog (the black dot indicates the location of rainfall centroid).

et al., 2017) is used as a basis for nonuniform spatial transposition. It is computed using a 2-D Gaussian kernel based on the locations of rainfall centroids for the 200 storms in the storm catalog (Figure 3b). Δx and Δy are then determined based on the spatial distribution from a 2-D Gaussian kernel.

Instead of assuming that the storm magnitude remains the same after transposition, a multiplicative ratio, termed an *intensity factor*, is developed based on the mean rainfall distribution of the storm catalog (Figure 3a). The transposed rainfall is given by

$$R_{\text{trans}} = \frac{r(x',y') * R_{(x,y)}}{r(x,y)} \quad (2)$$

where (x,y) is the original location of storm centroid and (x',y') is its transposed location. $r(x,y)$ and $r(x',y')$ are the rainfall values at location (x,y) and (x',y') , respectively, in the mean rainfall distribution map. $R_{(x,y)}$ and R_{trans} are the rainfall fields before and after transposition.

This step can be understood as generating a *synthetic year* of extreme rainfall events over the domain based on previous observations. For each of the k transposed storms, compute the t -hour basin-averaged rainfall depth that occurs over the watershed of interest. Among the k rainfall depths, the maximum is retained and can be understood as a synthetic t -hour annual rainfall maximum for the watershed.

The next step is to repeat the above steps to recreate multiple years of synthetic t -hour *annual* rainfall maxima for the watershed of interest. This repeated selection and analysis of subsets of data to make inferences is referred to in statistics as resampling. The SST methodology is used to

many locations the results of both are the products of *mixture distributions* (Smith, Villarini, et al., 2011) of storms with widely varying spatial and temporal rainfall scales that can interact with watershed and river channel properties to produce a spectrum of multiscale flood responses (ten Veldhuis et al., 2018; Wright, Smith, Villarini, et al., 2014; Zhou et al., 2017).

Tropical cyclone (TC) rainfall is identified using the HURDAT *best track* database from the National Oceanic and Atmospheric Administration (NOAA) National Hurricane Center (Jarvinen et al., 1984; Kaplan & DeMaria, 2003). Any rainfall occurring 12 h before to 12 h after a HURDAT storm track passes within 500 km of storm centroid is classified as tropical in origin. Hart and Evans (2001), Kunkel et al. (2010) and Zhou et al. (2017) use similar classification criteria for tropical cyclone rainfall.

Cloud-to-ground (CG) lightning observations are used to examine convective thunderstorm activity over the domain. CG lightning data are obtained from the National Lightning Detection Network (NLDN), which measures the time, location, polarity, peak current, and multiplicity of CG lightning flashes (see Orville (2008) for more details). CG lightning data have been used in previous studies for climatological analyses of thunderstorm activity over the United States e.g., Carey and Rutledge (2003); Bentley and Stallins (2005); Ntelekos et al. (2007); Villarini and Smith (2010); Yang et al. (2013). We classify the storm as a thunderstorm if there is more than one CG lightning strike recorded within 5 km of the storm center within a 3-hour time window around the t -hour time scale of storm.

2.5. Comparison of IDF Curves

We compare the SST estimates against intensity-duration-frequency (IDFs) from conventional rainfall frequency analyses, published as part of the Atlas 14 program by the NOAA (Bonnin et al., 2006). Regional L-moment frequency analysis (Hosking & Wallis, 1997) is the primary statistical method for this Atlas (see Bonnin et al., 2006, for details), and daily, hourly, and subhourly precipitation measurements were used. In Maryland, 74 daily, 16 hourly, and 2 subhourly stations are used for regional frequency analysis. The period of the data record in Atlas 14 is different from our study. The time periods of rain observations vary among the stations with the earliest record starting from 1891. In more than 50% stations, the records extend from the 1930s through the end of 2000. Atlas 14 provides point-scale estimates. Areal estimates are computed by obtaining multiplying the point estimate within Dead Run by the areal reduction factor (Bonnin et al., 2006). The area reduction factor is obtained the U.S. Weather Bureau Technical Paper No. 29 (U.S. Bureau, 1958). The relatively small size (14.3 km^2) of Dead Run means that the areal estimate is only slightly lower than the point estimate (as shown subsequently).

3. Results and Discussion

In this section, we first investigate the regional extreme rainfall heterogeneity through hydroclimatological analyses based on the storm catalogs and hydrometeorological analyses of two extreme storm events. The SST-based rainfall frequency analyses are then presented, focusing on the impact of spatial heterogeneity on rainfall estimation. Lastly, we carry out the sensitivity analysis to identify user-defined parameters of SST procedures that play significant roles in the results.

3.1. Storm Catalog Analyses

3.1.1. Spatial Heterogeneity of Rainfall

Spatial heterogeneity of extreme rainfall is characterized in terms of storm occurrence frequency and rainfall magnitude. A composite map of average storm total rainfall for the 200 events in the 3-hr storm catalog (Figure 3a) reveals a southwest-to-northeast spatial gradient in heavy rainfall activity across the domain, corresponding to an increasing spatial trend from inland to coastal areas. The maxima in occurrence frequency and mean rainfall is in the eastern portion of the study region between Baltimore city and Chesapeake Bay. Analyses of mean warm season rainfall (Smith et al., 1996; Smith et al., 2012) show a pronounced maximum in rainfall to the northeast (downwind) of Baltimore City. Downwind maxima in rainfall have been reported for a number of urban regions in United States (Niyogi et al., 2011; Shepherd, 2005; Wright et al., 2012; Wright, Smith, & Baeck, 2014). Mean rainfall varies by a factor of more than 5 over the domain for the 3-hr storm catalog, and occurrence frequency varies by a similar amount. The spatial probability of storm occurrence (Figure 3b) is computed using a 2-D Gaussian kernel based on the locations of rainfall centroids

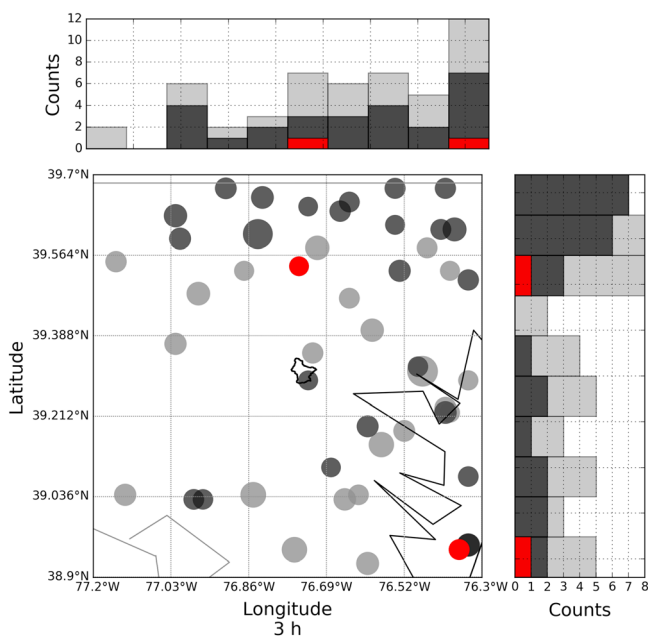


Figure 4. Location of the 50 most extreme storms in the 3-hr storm catalog, with tropical cyclones (red), thunderstorms (black), and all other storm types (gray). The dot size indicates the relative storm total rainfall with the scale and shape of Dead Run. The histograms indicate the storm counts in the east-west and north-south directions.

for each of the storms. A significant relationship is found between the spatial distribution of storm occurrence and average rainfall accumulation with a Spearman rank correlation over 0.8.

The pronounced spatial heterogeneity of extreme rainfall is closely linked to the complex topography in this area. Urban rainfall climatology can depend on regional features such as topography and land-water boundaries (Ntelekos et al., 2007; Ntelekos et al., 2008). As noted in section 2, the special terrain characteristics include the Chesapeake Bay in the east, mountainous terrain in the west, and urban land cover in and around the study area. The localized impacts of contrasts in topography and urban development, along with the land-water of Chesapeake Bay, play an important role in controlling regional extreme rainfall in the Baltimore region (Ntelekos et al., 2007; Ryu et al., 2016). The assumption of regional homogeneity, which was used in previous SST literature (Wright et al., 2013, 2017), is not appropriate in this study. In section 3.3.2, the impact of spatial heterogeneity will be further explored.

We further examine the spatial distribution of the 50 most extreme storms in storm catalogs, which are referred to as the extreme events. The location and magnitude of the 50 most extreme storms (Figure 4) exhibit similar spatial characteristics of regional extreme rainfall. There is an increasing trend in storm frequency from west to east, with no clear trend in the north-south direction. Only one storm centroid is within the Dead Run watershed. There is no clear spatial trend in rainfall intensity, which is similar to the results from the Charlotte area (Wright et al., 2013).

Among the 50 largest storms, there are 24 caused by warm-season thunderstorms, indicating the dominant role of thunderstorm in this area. Sixteen are located in the northern portion of the domain, close to the high-elevation area. This figure provides consistent results with the observation analysis in the Baltimore region (Ntelekos et al., 2007; Smith et al., 2012). There are only two tropical cyclones in the top 50 events. The seasonality and mechanism of storms will be detailed in sections 3.1.2 and 3.1.4. Results are similar for 1- and 6-hr storm catalogs (see the figures in supporting information).

3.1.2. Properties of Storm Occurrences

There is large interannual variability in storm counts for the 2000–2015 period. Figure 5a shows results for the 3-hr storm catalog. Twenty storms are from 2009, followed by 18 storms in 2000. Year 2002 has the fewest with six storms. The occurrences of the 50 largest storms show similar patterns. Though the distribution of interannual storm counts is highly variable, there is no obvious long-term trend in storm counts. The index of dispersion in annual storm counts, which is defined as the ratio of the variance to the mean, provides a measure to test the assumption of Poisson distribution. The index of dispersion is 1.33, pointing to

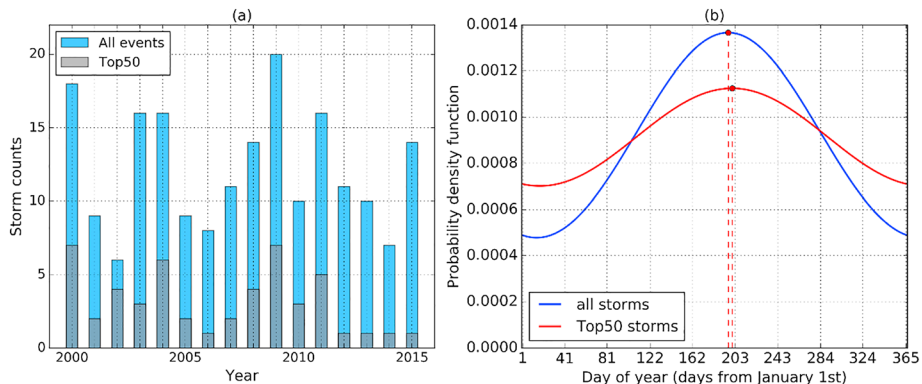


Figure 5. (a) Interannual distribution of storm counts and (b) intra-annual distribution of probability of storm occurrence in the 3-hr storm catalog.

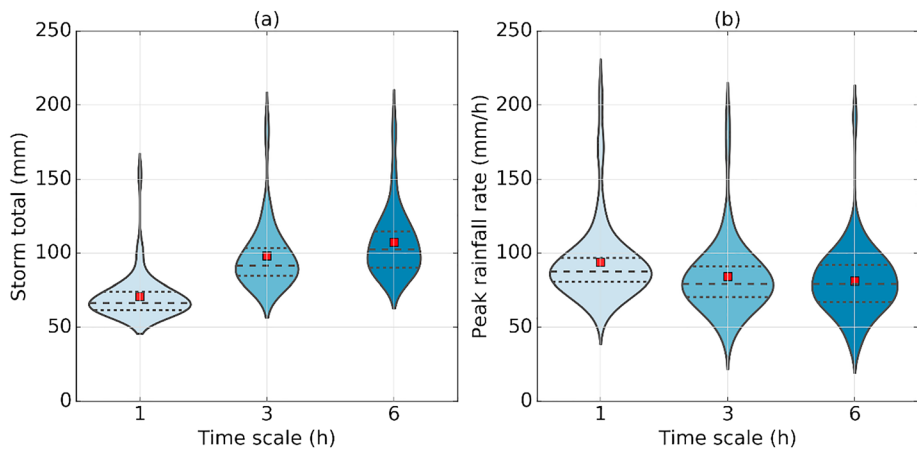


Figure 6. Violin plots of (a) storm total and (b) peak rainfall rates for the 50 most extreme storms in storm catalogs. (The red dot indicates mean value. Dashed line in the middle indicates the median value. Upper and lower dotted lines indicate 90th and 10th quantiles, respectively.)

overdispersed annual storm counts in the region. The 16-year sample size, however, precludes strong inferences, as well as the modeling of storm counts using other distributions, such as the negative binomial, which require relatively large sample sizes for accurate parameter estimation (e.g., Lloyd-Smith, 2007). Thus, in this study, we still follow the assumption used in most SST studies that the annual storm counts follow a Poisson distribution. The 1- and 6-hr catalogs exhibit similar properties (results not shown).

The storm occurrences in the 3-hr storm catalog show significant seasonality (Figure 5b). Frequency of storm occurrence for the 200 storms reveals a pronounced seasonal cycle with the peak in early June, highlighting the role of warm-season thunderstorms in the regional rainfall hydroclimatology. The seasonal distribution of the 50 largest storms is less *peaky* but with a similar seasonal maximum. Our results are consistent with other hydrometeorological analysis in the Baltimore region (Smith et al., 2012). There are fewer than 10 storms from October–March in each catalog, indicating that spring-winter extreme rainfall is infrequent in this region, at least at the spatial and temporal scales under consideration in this study. Results for the 1- and 6-hr catalogs are similar (see the figures in supporting information).

3.1.3. Properties of Rainfall Accumulations and Peak Rates

The DR-shaped storm total rainfall and the DR-shaped basin-averaged rainfall rates are calculated with the same size and shape of the Dead Run watershed. It should be noted that these storms did not actually occur in Dead Run. The distributions of the 50 largest storm total rainfall accumulations in 1-, 3-, and 6-hr storm catalogs are illustrated in Figure 6a. The median values are 66 mm at the 1-hr time scale, 92 mm at the 3-hr time scale, and 102 mm at the 6-hr time scale. The mean values are larger for each time scale, indicating right skew in the distributions. The kernel density distribution shows a slight multimodal trend with a small peak at the position greater than 75th quantile, indicating the existence of some extreme storms. In the 3-hr storm catalog, the largest 3-hr accumulation is 180 mm and the second largest is 179 mm, while the third largest storm is less than 140 mm. The variation in storm magnitude, represented by the coefficient of variation (the standard deviation divided by the mean), is similar at the three time scales (results not shown). In the top 10 events in the 6-hr storm catalog, 7 correspond to the same events that appear in the top 10 events in 3-hr storm catalog with similar storm magnitude. Furthermore, the two largest rainfall accumulations in the 3- and 6-hr time storm catalogs are produced by the same events and have similar storm total rainfall. This suggests that short-duration, high-intensity rain *bursts* embedded within longer-duration events can drive storm total accumulations in this region.

The distribution of maximum of *DR-shaped* basin-averaged rainfall rates shows features that differ from storm total rainfall accumulations (Figure 6b). The peak rainfall rates at the 1-hr time scale are larger, with a median of 88 mm/hr, while at the 3- and 6-hr time scale, the peak rainfall rates are comparable, both with median values of 79 mm/hr. The median values are close to the means at the 3- and 6-hr time scales, implying these distributions are not as right skewed. The small peak at the position greater than 75th quantile in the kernel density distribution is similar to the feature in storm total, showing the existence of high-

Table 1
Percent of Storms Produced by Tropical Cyclones and Thunderstorms

| Storm types | Duration (hr) | | |
|--|---------------|-----|-----|
| | 1 | 3 | 6 |
| Thunderstorms | 66% | 56% | 64% |
| Tropical cyclones | 3% | 3% | 3% |
| Number of thunderstorms in top 10 storms | 3 | 3 | 4 |

second largest event is the 27 May 2001 storm with 3-hr total of 177 mm. The storm centroid was close to the northern boundary of the domain. These are also the two largest storms in the 1-hr catalog.

Tropical cyclones account for less than 5% of all storm catalog entries (Table 1). Only two TCs appear within the top 50 storms in the 3-hr storm catalog: Hurricane Sandy on 29 October 2012 (3-hr storm total: 87 mm) in the southeast corner of domain and Hurricane Cindy on 7 July 2005 (3-hr storm total: 77 mm) in the northern portion of the domain. Hurricane Sandy ranks as the tenth largest storm in the 6-hr storm catalog with storm total of 120 mm. There are no tropical cyclone events in the storm catalog that are comparable in rainfall magnitude to Hurricane Agnes in June of 1972 (Bailey et al., 1975).

The two storm types reflect the mixtures within the extreme rainfall hydroclimatology in the Baltimore region, with warm-season thunderstorms playing a central role. In contrast with the previous study that shows that tropical cyclones are an important element of the upper tail of flood peak distributions in the Baltimore region (Smith, Villarini, et al., 2011; Villarini & Smith, 2010), however, we find that tropical cyclones are less important as rainfall generating mechanisms. The relatively low number of tropical cyclones in these storm catalogs reflects the fact that the 2000–2015 study period coincided with relatively few landfalling TC occurrences in the North Atlantic (Hall & Hereid, 2015; Hart et al., 2016). It is also likely that the TCs dominate over other storm types for long-duration (around 12–24 hr) storms, whereas for short-duration storms, the role of TCs is less important (Langousis & Veneziano, 2009). In section 3.4, the impact of storm types on SST estimates will be detailed.

3.1.5. Space-Time Structure of Rainfall

The correlation between storm total and peak rainfall rate decreases with increasing time scales (upper panels of Figure 7). At the 1-hr scale, the Spearman rank correlation coefficient is 0.57, showing relatively strong correlation between storm total and rainfall peak. At the 3-hr time scale, the correlation decreases

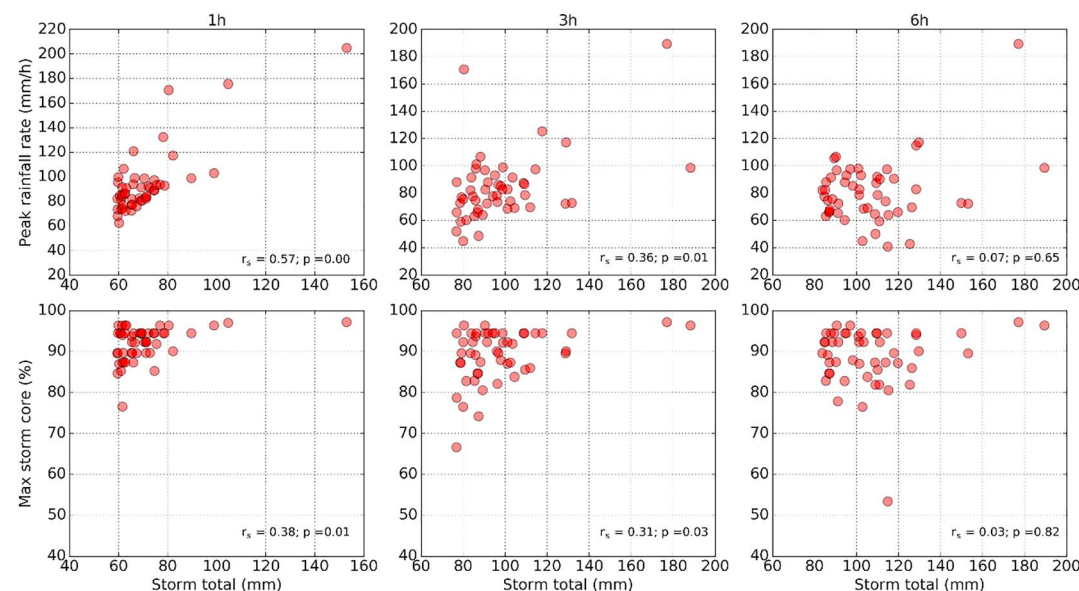


Figure 7. Scatterplot of storm total rainfall versus peak rainfall rate (upper panels), and maximum storm core coverage of the 50 most extreme storms in the 3-hr storm catalog (lower panels) with correlation (r_s) and p value (p).

magnitude values. The magnitude of extrema and the variability in peak rainfall rates are comparable among the three storm catalogs.

3.1.4. Mixture of Storm Types

Warm-season thunderstorms account for the largest fraction (>50%) of the 200 storms (Table 1), pointing to their prominent role in controlling the upper tail of extreme rainfall distribution. The largest storm in the 3-hr storm catalog is the thunderstorm system on 14 July 2000, which produced 188 mm over a DR-shaped area (see in section 3.2). The storm centroid was in the eastern part of the domain, near the Chesapeake Bay. The

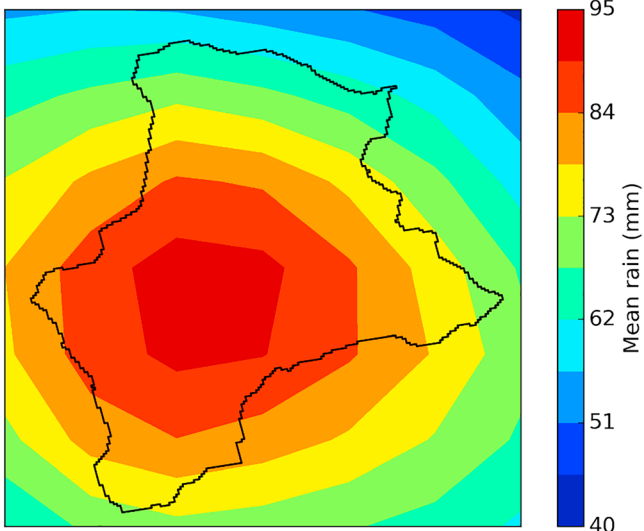


Figure 8. Composite map of mean storm total rainfall over the Dead Run-shaped watershed for the 200 storms in the 3-hr storm catalog.

to 0.36. The top two storms have similar storm total but contrasting peak rainfall rates, showing end-members, one with high-intensity rainfall rate and another with relatively lower rainfall rate but longer duration. At the 6-hr time scale, the relationship between rainfall peak and storm total is not significant.

We define *storm core coverage* as the percentage of the total number of radar grid cells (1 km^2) over the DR-shaped area (which constitutes 16 grid cells) that have rainfall intensity exceeding 25 mm/hr (see ten Veldhuis et al., 2018, for similar analysis), reflecting the spatial scale of the storm core relative to the watershed. The maximum storm core coverage over the DR-shaped area (lower panels of Figure 7) shows that the area of extreme rainfall rates varies at different time scales, even in a small (14.3 km^2) watershed. At the 1-hr time scale, except for one storm, all the top 50 storms have maximum storm core coverage greater than 80%, showing that at short time scale, major storms are capable of covering most of the DR-shaped area. At the 3- and 6-hr time scales, however, the storm core coverage shows larger variability, ranging from 50% to 98%. The correlation between storm total and maximum storm core coverage also decreases with increasing time scales. Differences in storm core coverage across time scales are linked to the different space-time structures of rainfall in the three storm catalogs.

The composite map (Figure 8) is the mean storm total of the 200 storms in the 3-hr storm catalog. It shows the spatial distribution of DR-shaped storms. Maximum rainfall is located approximately in the center of watershed area with a value exceeding 95 mm. Mean storm total rainfall decreases toward the watershed boundaries with the minimum magnitude of 60 mm in the northern boundary. Even in a 14.3-km^2 watershed, the spatial structure of storms is not uniform, providing a general map of spatial properties of extreme storms in the 3-hr storm catalog at relatively small spatial scale. The figure also implies an important advantage of SST, that is, to provide not only the IDF estimates but also the spatial structure of rainfall over the watershed.

3.2. Extreme Rainfall Case Studies

The upper tail of frequency analyses, whether based on SST or other techniques, is controlled by a relatively small number of extreme events in the period of record (Wright et al., 2013). Existing methods for diagnosing and accounting for heterogeneity in rainfall frequency analysis generally ignore physical hydrometeorological properties of these extreme events, instead proceeding directly to the resulting rainfall statistics. Here we examine two extreme storms to provide insights into storm properties that control upper-tail rainfall estimates. Both storms were embedded in environments with strong synoptic forcing, the first (14 July 2000) with an upper level trough to the west and the latter (12 August 2014) with a cold front moving through the region. To examine the storms in detail, the TITAN storm tracking algorithm (Dixon & Wiener, 1993) is used for analyses of the temporal evolution of echo top height and maximum reflectivity. CAPE (convective available potential energy) and precipitable water values are taken from the Sterling, Virginia radiosonde site.

The 14 July 2000 *Back Bay* storm (left panels of Figure 9) was embedded in a major severe weather outbreak in the mid-Atlantic region, producing extreme rainfall east of the Baltimore City. It also constitutes the largest storm in the 3- and 6-hr storm catalogs and second largest in the 1-hr catalog. There were no rain gauges in the area of most extreme rainfall and flooding; radar reveals maximum DR-shaped rainfall accumulations of 99, 188, and 189 mm at the 1-, 3-, and 6-hr time scales respectively occurred east of Baltimore City. The storm produced copious lightning, golf ball-sized hail, and damaging winds in the region. There were 1099 CG lightning strikes over the area in a 3-hr period. The prestorm environment was characterized by an unusually large CAPE value of $1,800 \text{ J/kg}$ and 36 mm of precipitable water. The heaviest rainfall and flooding for the July 2000 storm was east of Baltimore along the western margin of the Chesapeake Bay (upper left panel of Figure 9). In an environment in which most thunderstorms moved rapidly to the east-

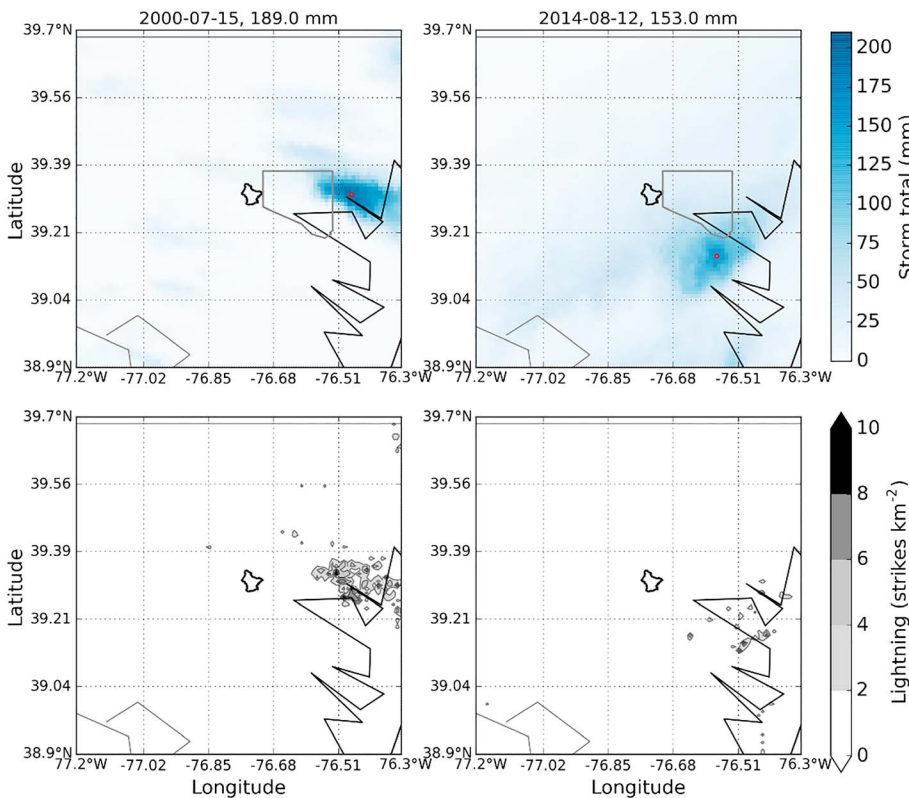


Figure 9. Spatial rainfall distribution (upper) and spatial lightning distribution (lower) for the 14 July 2000 storm and the 12 August 2014 storm. The red dots indicate the rainfall centroid of the storm.

northeast with steering level winds, the Back Bay storm remained quasi-stationary, as new cells repeatedly formed along the western margin of the existing storm element. Storm tracking analyses (Figure 10) show that from 21:00 to 23:00 UTC, the period of heaviest rainfall, net storm motion was small. During this time, maximum reflectivity reached 71 dBZ (Figure 10a) and echo top height reached 11.5 km. Propagation of the storm system balanced advection, resulting in extreme rainfall accumulations over the Back Bay region between Baltimore City and the bay. The heavy rain area is collocated with the maximum in CG lightning flash density (lower left panel of Figure 9), indicating that the heaviest rainfall was directly linked to the most intense convection.

The *Glen Burnie* storm of 12 August 2014 (upper right panel of Figure 9) was a weak thunderstorm embedded in a system that produced extreme rainfall in the mid-Atlantic region and record rainfall on Long Island in New York. This storm is the third largest in the 6-hr storm catalog. A rain gauge reported a peak storm total accumulation of 225 mm southeast of Baltimore City, close to the rainfall maximum shown by the radar. The largest 1-, 3-, and 6-hr rainfall accumulations of DR-shaped area for the August 2014 storm were 60, 129, and 153 mm, respectively. The prestorm environment for the August 2014 storm was characterized by a CAPE value of 430 J/kg and an unusually large precipitable water value of 49 mm at 0000 UTC on 12 August. The heaviest rainfall and heavy flooding for the August 2014 storm was southeast of Baltimore close to the western margin of the Chesapeake Bay. Most storm elements on 12 August 2014 moved to the northeast with the steering level flow. Like the Back Bay storm, the *Glen Burnie* storm remained virtually stationary for a period of approximately 2 hr and this period was responsible for the heaviest rainfall (Figure 10g). Echo top heights and maximum reflectivity values (Figure 10e) for the *Glen Burnie* storm were modest in comparison with the Back Bay storm, peaking at 7.5 km and 57.8 dBZ, respectively. Storm size for the Back Bay and *Glen Burnie* storms were comparable (Figures 10b and 10f), fluctuating around values of 120 km² during the period of peak rainfall. Size, storm motion, and rainfall rates for the two storms combined to produce spatial and temporal rainfall structures capable of producing extreme flooding in watersheds similar in size to Dead Run.

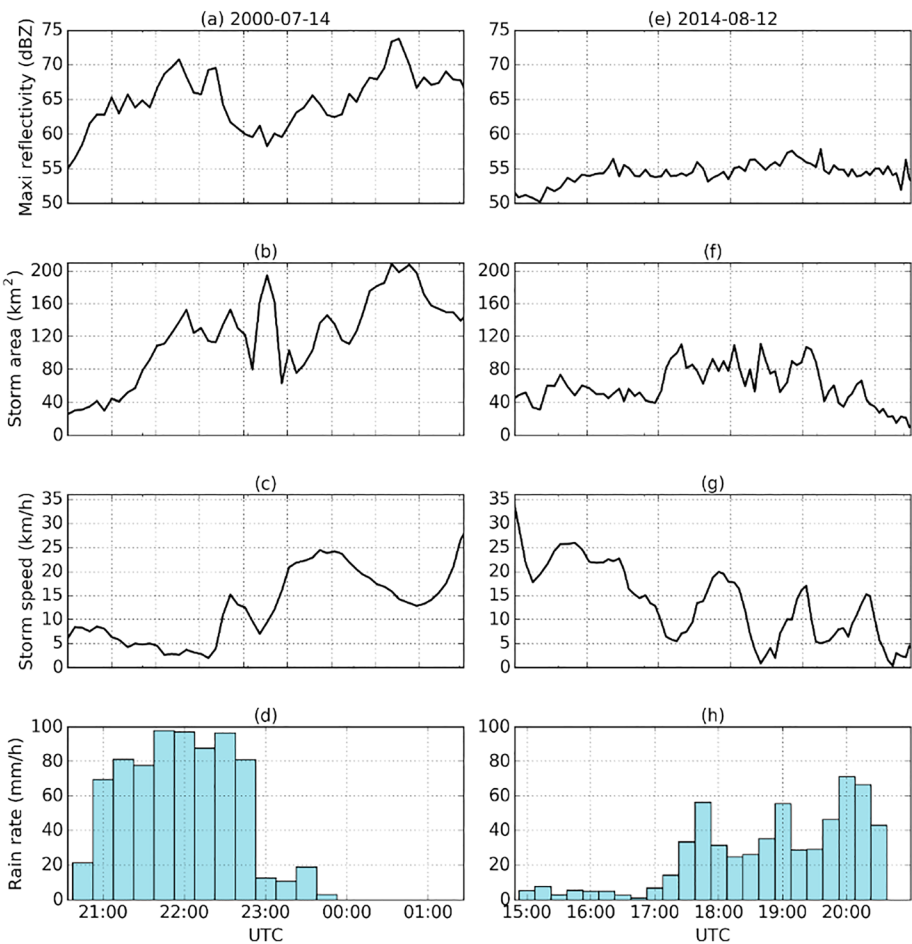


Figure 10. Time series of maximum reflectivity, storm area, storm speed, and rainfall rates for the 14 July 2000 storm (a–d) and the 12 August 2014 storm (e–h).

Extreme rainfall rates can be produced by intense convection or weak convection. For intense convection, storms with *collapsing* cells can produce especially large rainfall rates (see Smith, Baeck, et al., 2005; Smith et al., 2016; Yang et al., 2016). Weak convection and efficient warm rain precipitation processes have also been identified as important contributors to extreme rainfall rates and urban flooding (Petersen et al., 1999; Schumacher & Johnson, 2005). Warm near-surface air temperature improves the intensification of convective rain cells (Peleg et al., 2018). The contrasts in convective intensity and water vapor for the two storms show that diverse large-scale environmental *setups* can lead to extreme rainfall in the Baltimore region. It is likely that deeper understanding of current and future rainfall and flood frequency could be gained by further investigation of this range of *setup* conditions.

3.3. SST-Based Rainfall Frequency Analyses

3.3.1. Intensity-Duration-Frequency Curves

IDF curves with recurrence intervals from 5 to 500 years were generated using RainyDay software and the 1-, 3-, and 6-hr storm catalogs. One thousand SST realizations at each time scale were generated in order to examine the variability within frequency estimates for each return period. The original SST results without the intensity multiplier approach described in section 2.3 generally produce lower IDF estimates than NOAA Atlas 14 (left panels of Figure 11). Generally, 1- and 3-hr estimates show similar underestimation, which is more severe for return periods less than 50 years and tends to decrease for return periods greater than 100 years. At the 3-hr time scale, the two estimates agree well for the 500-year return period. At the 6-hr time scale, however, the underestimation is more significant, especially for return period greater than 50 years, where SST estimates are lower than the lower confidence level of Atlas 14 estimates.

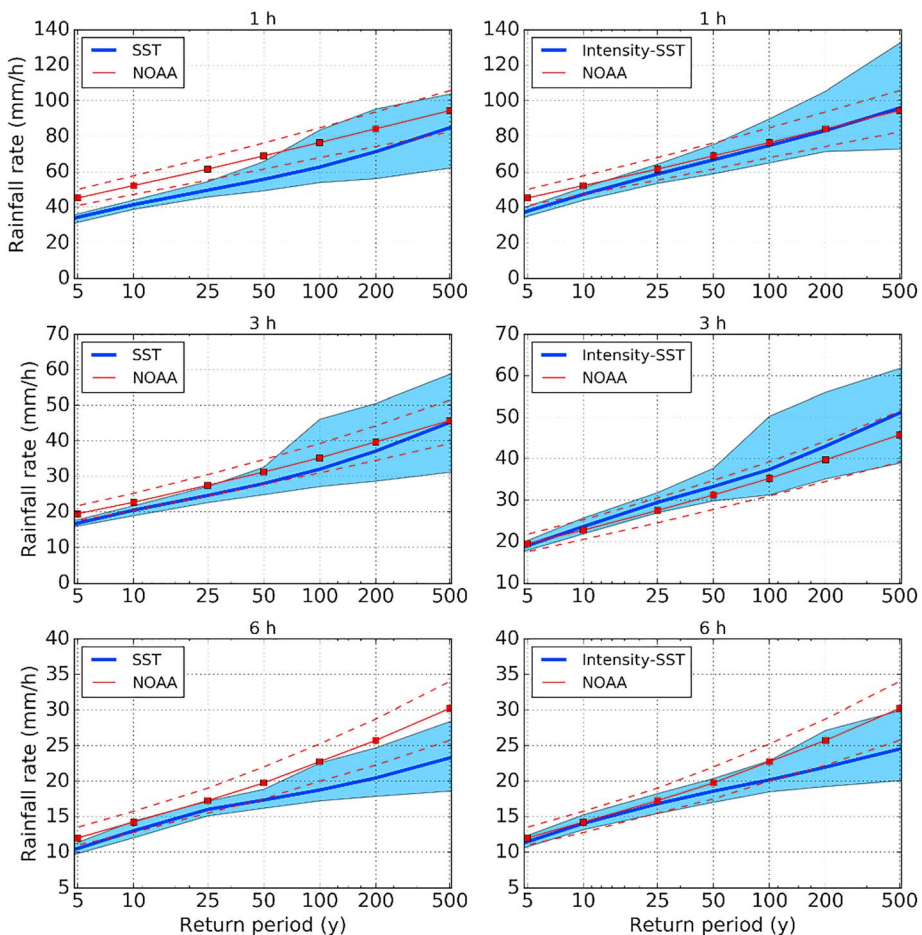


Figure 11. Comparison of intensity-duration-frequency curves from National Oceanic and Atmospheric Administration (NOAA) Atlas 14 to stochastic storm transposition (SST)-based curves generated using RainyDay (left column) and using RainyDay with the intensity multiplier approach (right column). The dashed red lines indicate the upper and lower confidence level of Atlas 14 estimates. The blue area indicates the spread of SST estimates with 90th and 10th quantiles as the solid gray line.

The SST results are generally larger with the intensity multiplier-based approach (right panels of Figure 11). At the 1-hr time scale, the intensity multiplier-based estimates tend to approach Atlas 14 with increasing return period. For the 500-year return period, the two estimates are similar. At the 3-hr time scale, the intensity multiplier-based estimates are higher than Atlas 14 except for the 5-year return period. For the 500-year return period, the intensity multiplier-based estimate is close to the 90% upper confidence level of Atlas 14. At the 6-hr time scale, the intensity multiplier-based estimates are still lower than Atlas 14, with its median value only close to the Atlas 14's lower confidence level.

The tendency for SST to underestimate more frequent event magnitudes has been reported in the literature (Foufoula-Georgiou, 1989; Franchini et al., 1996; Wilson & Foufoula-Georgiou, 1990; Wright et al., 2013). This can occur because it is relatively likely that for a given synthetic year, all k storms (see Step 4 of section 2.3) are transposed in such a way that little or no rainfall occurs over the watershed of interest, which is clearly unrealistic. Wright et al. (2013) argued that underestimation should be more prevalent for shorter duration storms and for smaller watersheds, since the geographic extent of the storms in the storm catalog will tend to be small relative to the transposition domain size. To mitigate this underestimation, Wright et al. (2017) suggested to enlarge the number of storms in the storm catalog. In our study, 200 storms are included in each storm catalog, which provides enough storms to avoid underestimation tied to storm sampling. The comparison of estimates using 200-event and 90-event storm catalogs will be detailed in section 3.4. The 6-hr underestimation for large return periods is associated with the relatively small number of tropical cyclones

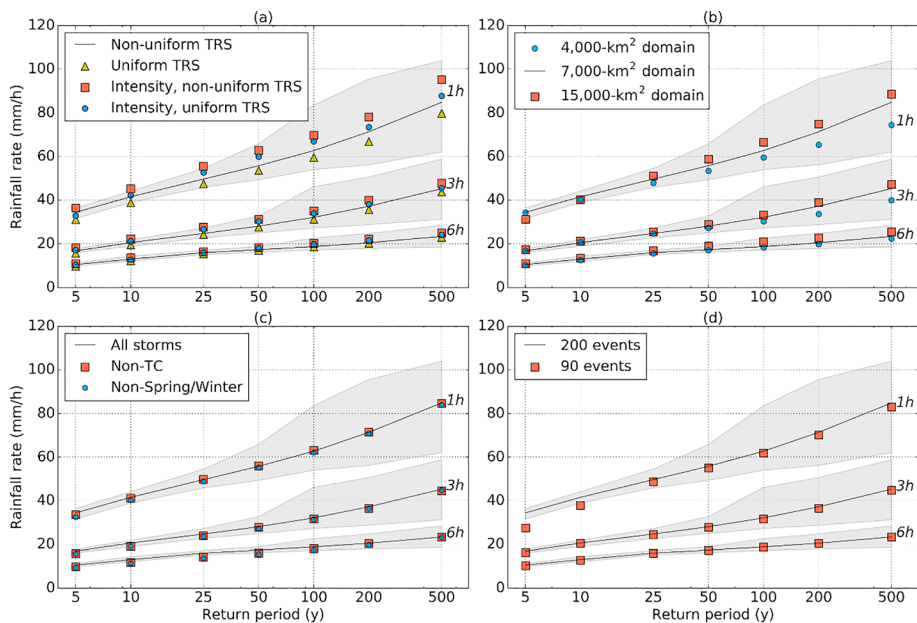


Figure 12. Comparison of intensity-duration-frequency (IDF) curves using (a) uniform/non-uniform TRS and intensity factor; (b) different domain sizes; (c) non-tropical cyclone (TC) and nonspring/winter storms; (d) catalog capacity of 90/200 events.

in the storm catalog (as discussed in section 3.1.4), which would potentially translate to lower IDF estimates for large return periods at longer rainfall durations.

We use the normalized interquartile range (NIR) to examine the variation of SST estimates. Similar to the ratio of the standard deviation to the mean, the NIR is the ratio of the interquartile range to the median, as a normalized measurement of the spread in estimates. The interquartile range is the difference between the 0.25 and 0.75 quantile. Generally, the variability in estimates increases with return period at each time scale (results not reported for the sake of brevity). For return periods less than 25 years, the variability in estimates is similar at the three time scales with the ratio less than 0.1. For return periods greater than 25 years, the NIR is comparable at the 1- and 3-hr time scales, while it is smallest at the 6-hr time scales. It demonstrates that the short-duration estimates have relatively larger variability than long-duration estimates.

3.3.2. Impact of Spatial Heterogeneity

The spatial heterogeneities in both storm occurrence and storm magnitude are examined through the comparison of SST estimates. We first compare IDF estimates using nonuniform spatial transposition (denoted as nonuniform TRS) to those using uniform transposition (denoted as uniform TRS). The comparison (Figure 12a) shows that the impact of storm occurrence is different at the three time scales. At the 1-hr time scale, nonuniform transposition results in higher IDF estimates for all return periods. The underestimation of uniform transposition decreases from 3- to 6-hr time scales. At the 6-hr time scale, the uniform and non-uniform transposition results are comparable except at the 5- and 10-year return periods. The results show that regional spatial heterogeneity impacts IDF estimates more significantly at shorter time scales.

We compare the uniform/nonuniform intensity factor-based estimates to the nonuniform transposition results (Figure 12a). As discussed in section 3.3.1, using the intensity factor, estimates are generally increased for all return periods at the three time scales. Nonuniform intensity factor-based results mostly produce larger estimates than uniform intensity-based results. Only at the 6-hr time scale and for return periods greater than 100 years are the two estimates consistent. The comparison confirms that the impact of spatial heterogeneity is significant at short time scales. The SST analysis also suggests important scale dependencies in regional spatial heterogeneity. Transposed storms could be extremely large when the intensity factor is anomalously large, which is obviously unrealistic. The intensity factor is a simplified method to account for the heterogeneity in rainfall magnitude. These results provide an initial demonstration that there are simple properties embedded within the rainfall observations themselves that can serve as a basis for the necessary transformations.

3.4. SST Sensitivity Analysis

Since several key features in the SST procedure are user defined, the analysis of sensitivity to these subjective parameters including transposition domain size, storm type, and storm catalog size, is undertaken to identify the parameters that most significantly impact the SST results.

3.4.1. Transposition Domain Area

We examine the impact of transposition area using three domain sizes: 4,000, 7,000, and 15,000 km² (Figure 12b). There is no systematic structure to the sensitivity of estimates using different domain sizes. For return periods smaller than 100 years, the differences in estimates using three domain sizes are not notable. For return periods larger than 100 years, the differences are somewhat larger. The estimates using 4,000 km² are the lowest among three domains, while the estimates using 7,000 and 15,000 km² are comparable in magnitudes. As noted in section 3.2, the upper tail of any rainfall frequency distribution is often controlled by a few of the most extreme storms in the observational record. In SST analysis, the large return period estimates come from transposed realizations of a few events from each storm catalog. For example, at the 3-hr time scale, for the 500-year return period, 83% of transposed storms are realizations derived from the 27 May 2001 storm, which occurred within both 7,000 and 15,000 km² domains. The finding confirms that estimation results are not strongly coupled to the domain size (Wright et al., 2013). This also implies that compared with the domain size, the existence and magnitude of extreme storms included in the domain area are more important factors in determining SST results. Enlarging the domain size can be an effective means of improving the sample representation of events in the upper tail of the rainfall distribution.

3.4.2. Storm Types

Other studies have shown that in the Baltimore region, both tropical cyclone and warm-season thunderstorms are important flash flood agents (Ntelekos et al., 2007; Smith & Smith, 2015). Because tropical cyclones can produce extreme rainfall magnitudes (Kunkel et al., 2010; Villarini et al., 2014), it is reasonable to assume that the tail estimates of extreme rainfall and flood frequency analyses will be influenced by TCs. Wright, Smith, & Baeck (2014) used SST and hydrologic modeling to show that TCs control the upper tail of flood risks in the Charlotte, North Carolina, in watersheds larger than 10 km².

To examine the impact of TCs on SST, the IDF estimates without tropical cyclones (denoted as non-TC) are compared to the results with all storms (Figure 12c). The estimates of non-TC and all storms are similar at the three time scales, except for those at 3- and 6-hr time scales with return periods smaller than 25 and 100 years, respectively. This modest contrast in estimates indicates the minor role of TCs in the SST estimates for Dead Run watershed during the 2000–2015 period. As noted above, the period of the radar data coincides with a period of low frequency TC, and thus, the SST-based IDF estimates may not reflect the underlying long-term role of TCs in the regional rainfall hydroclimatology. The long-term role of TCs can be assessed by using long-term gauge-based data set with lower resolution than radar rainfall field.

Similar results are found for winter/spring (October to March) storms (Figure 12c). Only at the 6-hr time scale do the estimates without winter/spring storms show lower estimates for return periods smaller than 200 years. This indicates that for time scales less than 6 hr, warm-season storms control the upper tail of the distribution of extreme rainfall, while at the 6-hr time scale, winter/spring storms are also capable of producing extreme rainfall. These results are related to the different space-time features between winter/spring storms and warm-season thunderstorms.

3.4.3. Size of Storm Catalog

The size of the storm catalog, that is, the number of storm events selected m , is important in describing regional extreme rainfall climatology. As argued in section 2.3, estimates can be less reliable when a relatively small number of storms are used. We compare the estimates using 200 events with those using only the 90 largest events (Figure 12d) in storm catalogs. The 90-event storm catalogs generally result in slight underestimation of estimates for small return periods; the severity of underestimation decreases with increasing duration. The estimates for return periods greater than 100 years, most of which are transpositions of 15 storms in the 30 largest storms, are not impacted by the less extreme storms. Thus, it is suggested to determine the capacity of storm catalog according to the design purpose. If we focus on the estimates for large return periods, smaller storm catalogs are suitable to produce reasonable estimates. But under a climatologically heterogeneous environment, oversized storm catalog will generate a less heterogeneous rainfall map (Figure 3) when using the intensity factor and thus impact the SST results. Additional analysis of larger

catalog size is suggested as future work to examine the sensitivity of more frequent (i.e., lower return period) estimates and the tradeoff between catalog size and heterogeneity.

4. Summary and Conclusions

In this study, we present an analysis of the spatially heterogeneous rainfall environment of the Baltimore Metropolitan region based on 16-year *storm catalogs* of extreme rainfall events derived from high-resolution (1-km², 15-min) radar rainfall fields. Principal conclusions of the study are as follows:

1. There is significant spatial heterogeneity in extreme rainfall across the Baltimore area. Spatial heterogeneity is closely linked to the complex terrain of the region, including the land-water boundary to the east, the mountainous terrain to the west, and the urban land use of Baltimore. Such fine-scale rainfall heterogeneities exist in many regions due to topographic and coastal features, and thus, the types of rainfall analyses presented here may be useful in other locations where radar rainfall data are available.
2. The transposition domain and storm catalogs are the foundation to reconstruct the climatology of extreme rainfall using SST. In this study, a 7,000-km² square domain is used to identify storms in the Baltimore region for inclusion in the storm catalogs. These catalogs contain the critical information regarding the regional climatology of extreme rainfall over relatively small spatial scales throughout the Baltimore region. Warm-season thunderstorm systems are shown to be the dominant mechanism for generating the intense, short-duration extreme rainfall that leads to flash flooding in this region.
3. The examination of two extreme rainfall events from the storm catalogs illustrate storm properties that control the upper tail of rainfall estimates. The different environments of the two storms show that both intense convection and weak convection can lead to extreme rainfall rates in the Baltimore region. The results provide insights to the hydrometeorological properties of extreme storms in the Baltimore region.
4. The SST procedure provides a viable method to address extreme rainfall spatial heterogeneity in rainfall frequency analysis (i.e., IDF) estimation. The original SST approach is expanded by applying a *multiplier field* that attempts to account for spatial heterogeneities in extreme rainfall magnitude. This method tends to increase IDF quantile estimates, particularly for short durations (1 and 3 hr). The apparent underestimation of SST at longer durations is linked to the low frequency of tropical cyclones during the study period. The storm catalogs do not include tropical cyclone events that are as severe as prior hurricanes that have produced extreme rainfall and flooding in the Baltimore region, most notably Hurricane Agnes in June 1972.
5. Like other frequency analysis approaches, estimates of the upper tail of the rainfall frequency distribution in the SST analyses are controlled by relatively few extreme events. IDF estimates for return periods larger than 200 years are transpositions of these few extreme storms in the storm catalog. The current SST procedure is effectively bounded by these events. Future research will address development of *random intensity factors* to address the impact of largest storms on the upper tail of the rainfall distribution.
6. Sensitivity analyses show that the SST results are dependent on several key features including the domain size, the rainfall duration, and the size of storm catalog. There is no systematic structure to the sensitivity of estimates using different domain sizes. A key idea of defining a domain is to capture the most extreme rainfall events that can be realistically transposed to the watershed of interest. Rainfall duration can be set with consideration of basin scale, storm type, and hydrologic response time properties. A smaller size storm catalog leads to lower estimates only for small return periods, which is consistent with previous studies.

SST, when coupled with a distributed hydrologic model, can be directly used for analyzing the frequency and severity of flooding. Such an approach yields advantages relative to other flood frequency analysis approaches, especially in urban areas. These advantages are discussed in Wright, Smith, Villarini, et al. (2014) but are briefly summarized here. High-resolution radar rainfall data combined with SST method yields extreme rainfall events with physically realistic rainfall space-time structure and motion, which are key determinants of flood frequency in urban areas (e.g., Peleg et al., 2017) and are essential for multiscale rainfall and flood frequency analysis. The ability of SST to estimate the tail of the extreme rainfall distribution from relatively short radar rainfall records and to provide these estimates as inputs to distributed hydrologic models presents opportunities for physically realistic flood frequency analysis in data-limited regions and in locations experiencing nonstationarities in rainfall or flooding due to climate change or

urbanization. This study contributes toward that goal by providing means for diagnosing and accounting for rainfall heterogeneity in such analyses.

Acknowledgments

The authors would like to acknowledge Geoff Pegram, Nadav Peleg, and the other anonymous reviewer for insightful comments and suggestions, which substantially improve the manuscript. This study was supported by the National Science Foundation (NSF grants CBET-144758 and AGS-1522492). D. Wright's contributions were supported by NSF Hydrologic Sciences CAREER grant EAR-1749638. The research is also supported by the China Initiative Postdocs Supporting Program and China Postdoctoral Science Foundation. Radar data are archived at Princeton University and can be downloaded from the url <http://arks.princeton.edu/ark:/88435/dsp01q524jr55d>.

References

- Alexander, G. (1963). Using the probability of storm transposition for estimating the frequency of rare floods. *Journal of Hydrology*, 1(1), 46–57. [https://doi.org/10.1016/0022-1694\(63\)90032-5](https://doi.org/10.1016/0022-1694(63)90032-5)
- Bailey, J. F., Patterson, J. L., & Paulhus, J. L. H. (1975). Hurricane Agnes rainfall and floods, June–July 1972.
- Beighley, R. E., & Moglen, G. E. (2002). Trend assessment in rainfall-runoff behavior in urbanizing watersheds. *Journal of Hydrologic Engineering*, 7(1), 27–34. [https://doi.org/10.1061/\(ASCE\)1084-0699\(2002\)7:1\(27\)](https://doi.org/10.1061/(ASCE)1084-0699(2002)7:1(27))
- Bentley, M. L., & Stallins, J. (2005). Climatology of cloud-to-ground lightning in Georgia, USA, 1992–2003. *International Journal of Climatology*, 25(15), 1979–1996. <https://doi.org/10.1002/joc.1227>
- Bonnin, G. M., Martin, D., Lin, B., Parzybok, T., Yekta, M., & Riley, D. (2006). NOAA Atlas 14: Precipitation-frequency atlas of the United States.
- Bureau, U. S. W. (1958). Rainfall intensity-frequency regime. Part 3-The middle Atlantic region, edited, U.S. Weather Bureau, Washington D. C.
- Carey, L. D., & Rutledge, S. A. (2003). Characteristics of cloud-to-ground lightning in severe and nonsevere storms over the Central United States from 1989–1998. *Journal of Geophysical Research*, 108(D15), 4483. <https://doi.org/10.1029/2002JD002951>
- Dawdy, D. R., Griffis, V. W., & Gupta, V. K. (2012). Regional flood-frequency analysis: How we got here and where we are going. *Journal of Hydrologic Engineering*, 17(9), 953–959. [https://doi.org/10.1061/\(ASCE\)HE.1943-5584.0000584](https://doi.org/10.1061/(ASCE)HE.1943-5584.0000584)
- Dixon, M., & Wiener, G. (1993). TITAN: Thunderstorm identification, tracking, analysis, and nowcasting—A radar-based methodology. *Journal of Atmospheric and Oceanic Technology*, 10(6), 785–797. [https://doi.org/10.1175/1520-0426\(1993\)010<0785:TTITAA>2.0.CO;2](https://doi.org/10.1175/1520-0426(1993)010<0785:TTITAA>2.0.CO;2)
- England, J. F., Julien, P. Y., & Velleux, M. L. (2014). Physically-based extreme flood frequency with stochastic storm transposition and paleoflood data on large watersheds. *Journal of Hydrology*, 510, 228–245. <https://doi.org/10.1016/j.jhydrol.2013.12.021>
- Fontaine, T. A., & Potter, K. W. (1989). Estimating probabilities of extreme rainfalls. *Journal of Hydraulic Engineering*, 115(11), 1562–1575. [https://doi.org/10.1061/\(ASCE\)0733-9429\(1989\)115:11\(1562\)](https://doi.org/10.1061/(ASCE)0733-9429(1989)115:11(1562))
- Foufoula-Georgiou, E. (1989). A probabilistic storm transposition approach for estimating exceedance probabilities of extreme precipitation depths. *Water Resources Research*, 25, 799–815. <https://doi.org/10.1029/WR025i005p00799>
- Franchini, M., Helmlinger, K., Foufoula-Georgiou, E., & Todini, E. (1996). Stochastic storm transposition coupled with rainfall-runoff modeling for estimation of exceedance probabilities of design floods. *Journal of Hydrology*, 175(1–4), 511–532. [https://doi.org/10.1016/S0022-1694\(96\)80022-9](https://doi.org/10.1016/S0022-1694(96)80022-9)
- Fulton, R. A., Breidenbach, J. P., Seo, D.-J., Miller, D. A., & O'Bannon, T. (1998). The WSR-88D rainfall algorithm. *Weather and Forecasting*, 13(2), 377–395. [https://doi.org/10.1175/1520-0434\(1998\)013<0377:TWRA>2.0.CO;2](https://doi.org/10.1175/1520-0434(1998)013<0377:TWRA>2.0.CO;2)
- Groffman, P. M., Bain, D. J., Band, L. E., Belt, K. T., Brush, G. S., Grove, J. M., et al. (2003). Down by the riverside: Urban riparian ecology. *Frontiers in Ecology and the Environment*, 1(6), 315–321. [https://doi.org/10.1890/1540-9295\(2003\)001\[0315:DBTR\]2.0.CO;2](https://doi.org/10.1890/1540-9295(2003)001[0315:DBTR]2.0.CO;2)
- Gupta, V. K. (1972). Transposition of storms for estimating flood probability distributions, hydrology papers (Colorado State University); no. 59.
- Hall, T., & Hereid, K. (2015). The frequency and duration of US hurricane droughts. *Geophysical Research Letters*, 42, 3482–3485. <https://doi.org/10.1002/2015GL063652>
- Hamidi, A., Devineni, N., Booth, J. F., Hosten, A., Ferraro, R. R., & Khanbilvardi, R. (2017). Classifying urban rainfall extremes using weather radar data: An application to the greater New York area. *Journal of Hydrometeorology*, 18(3), 611–623. <https://doi.org/10.1175/JHM-D-16-0193.1>
- Hart, R. E., Chavas, D. R., & Guishard, M. P. (2016). The arbitrary definition of the current Atlantic major hurricane landfall drought. *Bulletin of the American Meteorological Society*, 97(5), 713–722. <https://doi.org/10.1175/BAMS-D-15-00185.1>
- Hart, R. E., & Evans, J. L. (2001). A climatology of the extratropical transition of Atlantic tropical cyclones. *Journal of Climate*, 14(4), 546–564. [https://doi.org/10.1175/1520-0442\(2001\)014<0546:ACOTET>2.0.CO;2](https://doi.org/10.1175/1520-0442(2001)014<0546:ACOTET>2.0.CO;2)
- Hosking, J. R. M., & Wallis, J. R. (1997). *Regional frequency analysis: An approach based on L-moments*. Cambridge, UK: Cambridge University Press. <https://doi.org/10.1017/CBO9780511529443>
- Jarvinen, B., Neumann, C., & Davis, M. (1984). A tropical cyclone data tape for the North Atlantic Basin, 1886–1983: Contents, limitations, and Uses.
- Javier, J. R. N., Smith, J. A., Meierdiercks, K. L., Baeck, M. L., & Miller, A. J. (2007). Flash flood forecasting for small urban watersheds in the Baltimore metropolitan region. *Weather and Forecasting*, 22(6), 1331–1344. <https://doi.org/10.1175/2007WAF2006036.1>
- Kaplan, J., & DeMaria, M. (2003). Large-scale characteristics of rapidly intensifying tropical cyclones in the North Atlantic basin. *Weather and Forecasting*, 18(6), 1093–1108. [https://doi.org/10.1175/1520-0434\(2003\)018<1093:LCORIT>2.0.CO;2](https://doi.org/10.1175/1520-0434(2003)018<1093:LCORIT>2.0.CO;2)
- Khaliq, M. N., Ouarda, T. B. M. J., Ondo, J. C., Gachon, P., & Bobée, B. (2006). Frequency analysis of a sequence of dependent and/or non-stationary hydro-meteorological observations: A review. *Journal of Hydrology*, 329(3–4), 534–552. <https://doi.org/10.1016/j.jhydrol.2006.03.004>
- Krajewski, W. F., Kruger, A., Smith, J. A., Lawrence, R., Gunyon, C., Goska, R., et al. (2011). Towards better utilization of NEXRAD data in hydrology: An overview of Hydro-NEXRAD. *Journal of Hydroinformatics*, 13(2), 255–266. <https://doi.org/10.2166/hydro.2010.056>
- Kunkel, K. E., Easterling, D. R., Kristovich, D. A., Gleason, B., Stoecker, L., & Smith, R. (2010). Recent increases in US heavy precipitation associated with tropical cyclones. *Geophysical Research Letters*, 37, L24706. <https://doi.org/10.1029/2010GL045164>
- Langousis, A., & Veneziano, D. (2009). Long-term rainfall risk from tropical cyclones in coastal areas. *Water Resources Research*, 45, W11430. <https://doi.org/10.1029/2008WR007624>
- Lin, N., Smith, J. A., Villarini, G., Marchok, T. P., & Baeck, M. L. (2010). Modeling extreme rainfall, winds, and surge from Hurricane Isabel (2003). *Weather and Forecasting*, 25(5), 1342–1361. <https://doi.org/10.1175/2010WAF2222349.1>
- Lloyd-Smith, J. O. (2007). Maximum likelihood estimation of the negative binomial dispersion parameter for highly overdispersed data, with applications to infectious diseases. *PLoS One*, 2(2), e180. <https://doi.org/10.1371/journal.pone.0000180>
- Meierdiercks, K. L., Smith, J. A., Baeck, M. L., & Miller, A. J. (2010). Analyses of urban drainage network structure and its impact on hydrologic response. *JAWRA Journal of the American Water Resources Association*, 46(5), 932–943. <https://doi.org/10.1111/j.1752-1688.2010.00465.x>

- Milly, P. C., Betancourt, J., Falkenmark, M., Hirsch, R. M., Kundzewicz, Z. W., Lettenmaier, D. P., & Stouffer, R. J. (2008). Stationarity is dead: Whither water management? *Science*, 319(5863), 573–574. <https://doi.org/10.1126/science.1151915>
- Morin, E., Goodrich, D. C., Maddox, R. A., Gao, X., Gupta, H. V., & Sorooshian, S. (2006). Spatial patterns in thunderstorm rainfall events and their coupling with watershed hydrological response. *Advances in Water Resources*, 29(6), 843–860. <https://doi.org/10.1016/j.advwatres.2005.07.014>
- Nathan, R., Jordan, P., Scorah, M., Lang, S., Kuczera, G., Schaefer, M., & Weinmann, E. (2016). Estimating the exceedance probability of extreme rainfalls up to the probable maximum precipitation. *Journal of Hydrology*, 543, 706–720. <https://doi.org/10.1016/j.jhydrol.2016.10.044>
- Nelson, P. A., Smith, J. A., & Miller, A. J. (2006). Evolution of channel morphology and hydrologic response in an urbanizing drainage basin. *Earth Surface Processes and Landforms*, 31(9), 1063–1079. <https://doi.org/10.1002/esp.1308>
- Niyogi, D., Pyle, P., Lei, M., Arya, S. P., Kishtawal, C. M., Shepherd, M., et al. (2011). Urban modification of thunderstorms: An observational storm climatology and model case study for the Indianapolis urban region. *Journal of Applied Meteorology and Climatology*, 50(5), 1129–1144. <https://doi.org/10.1175/2010JAMC1836.1>
- Norbiato, D., Borga, M., Sangati, M., & Zanon, F. (2007). Regional frequency analysis of extreme precipitation in the eastern Italian Alps and the August 29, 2003 flash flood. *Journal of Hydrology*, 345(3–4), 149–166. <https://doi.org/10.1016/j.jhydrol.2007.07.009>
- Ntelekos, A. A., Smith, J. A., Baeck, M. L., Krajewski, W. F., Miller, A. J., & Goska, R. (2008). Extreme hydrometeorological events and the urban environment: Dissecting the 7 July 2004 thunderstorm over the Baltimore MD Metropolitan Region. *Water Resources Research*, 44, W08446. <https://doi.org/10.1029/2007WR006346>
- Ntelekos, A. A., Smith, J. A., & Krajewski, W. F. (2007). Climatological analyses of thunderstorms and flash floods in the Baltimore Metropolitan Region. *Journal of Hydrometeorology*, 8(1), 88–101. <https://doi.org/10.1175/JHM558.1>
- Ogden, F. L., Sharif, H. O., Senarath, S. U. S., Smith, J. A., Baeck, M. L., & Richardson, J. R. (2000). Hydrologic analysis of the Fort Collins, Colorado, flash flood of 1997. *Journal of Hydrology*, 228(1–2), 82–100. [https://doi.org/10.1016/S0022-1694\(00\)00146-3](https://doi.org/10.1016/S0022-1694(00)00146-3)
- Orville, R. E. (2008). Development of the national lightning detection network. *Bulletin of the American Meteorological Society*, 89(2), 180–190. <https://doi.org/10.1175/BAMS-89-2-180>
- Peleg, N., Blumensaat, F., Molnar, P., Faticchi, S., & Burlando, P. (2017). Partitioning the impacts of spatial and climatological rainfall variability in urban drainage modeling. *Hydrology and Earth System Sciences*, 21(3), 1559–1572. <https://doi.org/10.5194/hess-21-1559-2017>
- Peleg, N., Marra, F., Faticchi, S., Molnar, P., Morin, E., Sharma, A., & Burlando, P. (2018). Intensification of convective rain cells at warmer temperatures observed from high-resolution weather radar data. *Journal of Hydrometeorology*, 19(4), 715–726. <https://doi.org/10.1175/JHM-D-17-0158.1>
- Petersen, W. A., Carey, L. D., Rutledge, S. A., Knivele, J. C., Johnson, R. H., Doesken, N. J., et al. (1999). Mesoscale and radar observations of the Fort Collins flash flood of 28 July 1997. *Bulletin of the American Meteorological Society*, 80(2), 191–216. [https://doi.org/10.1175/1520-0477\(1999\)080<0191:MAROOT>2.0.CO;2](https://doi.org/10.1175/1520-0477(1999)080<0191:MAROOT>2.0.CO;2)
- Ramos, M. H., Creutin, J.-D., & Leblouis, E. (2005). Visualization of storm severity. *Journal of Hydrology*, 315(1–4), 295–307. <https://doi.org/10.1016/j.jhydrol.2005.04.007>
- Reger, J. P., & Cleaves, E. T. (2008). Explanatory text for the physio-graphic map of Maryland.
- Ryu, Y.-H., Smith, J. A., Bou-Zeid, E., & Baeck, M. L. (2016). The influence of land surface heterogeneities on heavy convective rainfall in the Baltimore–Washington metropolitan area. *Monthly Weather Review*, 144(2), 553–573. <https://doi.org/10.1175/MWR-D-15-0192.1>
- Schumacher, R. S., & Johnson, R. H. (2005). Organization and environmental properties of extreme-rain-producing mesoscale convective systems. *Monthly Weather Review*, 133(4), 961–976. <https://doi.org/10.1175/MWR2899.1>
- Seo, B.-C., Krajewski, W. F., Kruger, A., Domaszynski, P., Smith, J. A., & Steiner, M. (2011). Radar-rainfall estimation algorithms of Hydro-NEXRAD. *Journal of Hydroinformatics*, 13(2), 277–291. <https://doi.org/10.2166/hydro.2010.003>
- Seo, D.-J., & Breidenbach, J. (2002). Real-time correction of spatially nonuniform bias in radar rainfall data using rain gauge measurements. *Journal of Hydrometeorology*, 3(2), 93–111. [https://doi.org/10.1175/1525-7541\(2002\)003<0093:RTCOSN>2.0.CO;2](https://doi.org/10.1175/1525-7541(2002)003<0093:RTCOSN>2.0.CO;2)
- Shepherd, J. M. (2005). A review of current investigations of urban-induced rainfall and recommendations for the future. *Earth Interactions*, 9(12), 1–27. <https://doi.org/10.1175/EI156.1>
- Smith, B., Smith, J., Baeck, M., & Miller, A. (2015). Exploring storage and runoff generation processes for urban flooding through a physically based watershed model. *Water Resources Research*, 51, 1552–1569. <https://doi.org/10.1002/2014WR016085>
- Smith, B. K., Smith, J., & Baeck, M. L. (2016). Flash flood-producing storm properties in a small urban watershed. *Journal of Hydrometeorology*, 7(2016), 2631–2647.
- Smith, B. K., & Smith, J. A. (2015). The flashiest watersheds in the contiguous United States. *Journal of Hydrometeorology*, 16(6), 2365–2381. <https://doi.org/10.1175/JHM-D-14-0217.1>
- Smith, J. A., Baeck, M. L., Meierdiercks, K. L., Miller, A. J., & Krajewski, W. F. (2007). Radar rainfall estimation for flash flood forecasting in small urban watersheds. *Advances in Water Resources*, 30(10), 2087–2097. <https://doi.org/10.1016/j.advwatres.2006.09.007>
- Smith, J. A., Baeck, M. L., Meierdiercks, K. L., Nelson, P. A., Miller, A. J., & Holland, E. J. (2005). Field studies of the storm event hydrologic response in an urbanizing watershed. *Water Resources Research*, 41, W10413. <https://doi.org/10.1029/2004WR003712>
- Smith, J. A., Baeck, M. L., Morrison, J. E., Sturdevant-Rees, P., Turner-Gillespie, D. F., & Bates, P. D. (2002). The regional hydrology of extreme floods in an urbanizing drainage basin. *Journal of Hydrometeorology*, 3(3), 267–282. [https://doi.org/10.1175/1525-7541\(2002\)003<0267:TRHOEF>2.0.CO;2](https://doi.org/10.1175/1525-7541(2002)003<0267:TRHOEF>2.0.CO;2)
- Smith, J. A., Baeck, M. L., Ntelekos, A. A., Villarini, G., & Steiner, M. (2011). Extreme rainfall and flooding from orographic thunderstorms in the central Appalachians. *Water Resources Research*, 47, W04514. <https://doi.org/10.1029/2010WR010190>
- Smith, J. A., Baeck, M. L., Steiner, M., & Miller, A. J. (1996). Catastrophic rainfall from an upslope thunderstorm in the central Appalachians: The Rapidan storm of June 27, 1995. *Water Resources Research*, 32, 3099–3113. <https://doi.org/10.1029/96WR02107>
- Smith, J. A., Baeck, M. L., Villarini, G., Welty, C., Miller, A. J., & Krajewski, W. F. (2012). Analyses of a long-term, high-resolution radar rainfall data set for the Baltimore metropolitan region. *Water Resources Research*, 48, W04504. <https://doi.org/10.1029/2011WR010641>
- Smith, J. A., & Krajewski, W. F. (1991). Estimation of the mean field bias of radar rainfall estimates. *Journal of Applied Meteorology*, 30(4), 397–412. [https://doi.org/10.1175/1520-0450\(1991\)030<0397:EOTMFB>2.0.CO;2](https://doi.org/10.1175/1520-0450(1991)030<0397:EOTMFB>2.0.CO;2)
- Smith, J. A., Miller, A. J., Baeck, M. L., Nelson, P. A., Fisher, G. T., & Meierdiercks, K. L. (2005). Extraordinary flood response of a small urban watershed to short-duration convective rainfall. *Journal of Hydrometeorology*, 6(5), 599–617. <https://doi.org/10.1175/JHM426.1>
- Smith, J. A., Villarini, G., & Baeck, M. L. (2011). Mixture distributions and the hydroclimatology of extreme rainfall and flooding in the eastern United States. *Journal of Hydrometeorology*, 12(2), 294–309. <https://doi.org/10.1175/2010JHM1242.1>

- Suyanto, A., O'Connell, P., & Metcalfe, A. (1995). The influence of storm characteristics and catchment conditions on extreme flood response: A case study based on the brue river basin, UK. *Surveys in Geophysics*, 16(2), 201–225. <https://doi.org/10.1007/BF00665780>
- Tarolli, M., Borga, M., Zoccatelli, D., Bernhofer, C., Jatho, N., & Janabi, F. a. (2013). Rainfall space-time organization and orographic control on flash flood response: The Weisseritz event of August 13, 2002. *Journal of Hydrologic Engineering*, 18(2), 183–193. [https://doi.org/10.1061/\(ASCE\)HE.1943-5584.0000569](https://doi.org/10.1061/(ASCE)HE.1943-5584.0000569)
- ten Veldhuis, M. C., Zhou, Z., Yang, L., Liu, S., & Smith, J. (2018). The role of storm scale, position and movement in controlling urban flood response. *Hydrology and Earth System Sciences*, 22(1), 417–436. <https://doi.org/10.5194/hess-22-417-2018>
- Thorndahl, S., Smith, J. A., Baeck, M. L., & Krajewski, W. F. (2014). Analyses of the temporal and spatial structures of heavy rainfall from a catalog of high-resolution radar rainfall fields. *Atmospheric Research*, 144, 111–125. <https://doi.org/10.1016/j.atmosres.2014.03.013>
- Villarini, G., Goska, R., Smith, J. A., & Vecchi, G. A. (2014). North Atlantic tropical cyclones and U.S. flooding. *Bulletin of the American Meteorological Society*, 95(9), 1381–1388. <https://doi.org/10.1175/BAMS-D-13-00060.1>
- Villarini, G., & Krajewski, W. F. (2010). Review of the different sources of uncertainty in single polarization radar-based estimates of rainfall. *Surveys in Geophysics*, 31(1), 107–129. <https://doi.org/10.1007/s10712-009-9079-x>
- Villarini, G., & Smith, J. A. (2010). Flood peak distributions for the eastern United States. *Water Resources Research*, 46, W06504. <https://doi.org/10.1029/2009WR008395>
- Villarini, G., Smith, J. A., Baeck, M. L., Smith, B. K., & Sturdevant-Rees, P. (2013). Hydrologic analyses of the July 17–18, 1996, flood in Chicago and the role of urbanization. *Journal of Hydrologic Engineering*, 18(2), 250–259. [https://doi.org/10.1061/\(ASCE\)HE.1943-5584.0000462](https://doi.org/10.1061/(ASCE)HE.1943-5584.0000462)
- Villarini, G., Smith, J. A., Lynn Baeck, M., Sturdevant-Rees, P., & Krajewski, W. F. (2010). Radar analyses of extreme rainfall and flooding in urban drainage basins. *Journal of Hydrology*, 381(3–4), 266–286. <https://doi.org/10.1016/j.jhydrol.2009.11.048>
- Volkmann, T. H., Lyon, S. W., Gupta, H. V., & Troch, P. A. (2010). Multicriteria design of rain gauge networks for flash flood prediction in semiarid catchments with complex terrain. *Water Resources Research*, 46, W11554. <https://doi.org/10.1029/2010WR009145>
- Welty, C., Miller, A. J., Belt, K. T., Smith, J. A., Band, L. E., Groffman, P. M., et al. (2007). Design of an environmental field observatory for quantifying the urban water budget. In V. Novotny & P. Brown (Eds.), *Cities of the future: Towards integrated sustainable water and landscape management* (p. 7491). London, UK: IWA Publishing.
- Wilson, L. L., & Foufoula-Georgiou, E. (1990). Regional rainfall frequency analysis via stochastic storm transposition. *Journal of Hydraulic Engineering*, 116(7), 859–880. [https://doi.org/10.1061/\(ASCE\)0733-9429\(1990\)116:7\(859\)](https://doi.org/10.1061/(ASCE)0733-9429(1990)116:7(859))
- Wright, D. B., Mantilla, R., & Peters-Lidard, C. D. (2017). A remote sensing-based tool for assessing rainfall-driven hazards. *Environmental Modelling & Software*, 90, 34–54. <https://doi.org/10.1016/j.envsoft.2016.12.006>
- Wright, D. B., Smith, J. A., & Baeck, M. L. (2014). Flood frequency analysis using radar rainfall fields and stochastic storm transposition. *Water Resources Research*, 50, 1592–1615. <https://doi.org/10.1002/2013WR014224>
- Wright, D. B., Smith, J. A., Villarini, G., & Baeck, M. L. (2012). Hydroclimatology of flash flooding in Atlanta. *Water Resources Research*, 48, W04524. <https://doi.org/10.1029/2011WR011371>
- Wright, D. B., Smith, J. A., Villarini, G., & Baeck, M. L. (2013). Estimating the frequency of extreme rainfall using weather radar and stochastic storm transposition. *Journal of Hydrology*, 488, 150–165. <https://doi.org/10.1016/j.jhydrol.2013.03.003>
- Wright, D. B., Smith, J. A., Villarini, G., & Baeck, M. L. (2014). Long-term high-resolution radar rainfall fields for urban hydrology. *Journal of the American Water Resources Association*, 50(3), 713–734. <https://doi.org/10.1111/jawr.12139>
- Yang, L., Smith, J. A., Baeck, M. L., & Zhang, Y. (2016). Flash flooding in small urban watersheds: Storm event hydrologic response. *Water Resources Research*, 52, 4571–4589. <https://doi.org/10.1002/2015WR018326>
- Yang, L., Smith, J. A., Wright, D. B., Baeck, M. L., Villarini, G., Tian, F., & Hu, H. (2013). Urbanization and climate change: An examination of nonstationarities in urban flooding. *Journal of Hydrometeorology*, 14(6), 1791–1809. <https://doi.org/10.1175/JHM-D-12-095.1>
- Yang, L., Tian, F., Smith, J. A., & Hu, H. (2014). Urban signatures in the spatial clustering of summer heavy rainfall events over the Beijing metropolitan region. *Journal of Geophysical Research: Atmospheres*, 119, 1203–1217. <https://doi.org/10.1002/2013JD020762>
- Zhou, Z., Smith, J. A., Yang, L., Baeck, M. L., Chaney, M., Ten Veldhuis, M.-C., et al. (2017). The complexities of urban flood response: Flood frequency analyses for the Charlotte Metropolitan Region. *Water Resources Research*, 53, 7401–7425. <https://doi.org/10.1002/2016WR019997>